AGU PUBLICATIONS

Global Biogeochemical Cycles

Supporting Information for

Spatiotemporal characterization of mercury isotope baselines and anthropogenic influences in lake sediment cores

Ju Hyeon Lee[1], Sae Yun Kwon[1,2*], Runsheng Yin[3], Laura M. Motta[1], Aaron Y. Kurz[4], Seung-Il Nam[5]

[1] Division of Environmental Science and Engineering, Pohang University of Science and Technology, 77 Cheongam-Ro, Nam Gu, Pohang 37673 South Korea

[2] Institute for Convergence Research and Education in Advanced Technology, Yonsei University, 85 Songdogwahak-Ro, Yeonsu-Gu, Incheon 21983 South Korea

[3] State Key Laboratory of Ore Deposit Geochemistry, Institute of Geochemistry, Chinese Academy of Sciences, 99 West Lincheng Road, Guiyang, Guizhou 550081 China

[4] Department of Earth and Environmental Sciences, University of Michigan, 1100 N. University Avenue, Ann Arbor, Michigan 48109 United States

[5] Division of Polar Paleoenvironment, Korea Polar Research Institute, 260 Songdomirae-ro, Yeonsu-gu, Incheon 21990 South Korea

* Corresponding author: Sae Yun Kwon (saeyunk@postech.ac.kr)

Contents of this file

Tables S1 to S7
Figures S1 to S3

Introduction

The supporting information contains seven tables and three figures to show various additional analysis conducted to interpret the compiled mercury concentration (THg) and mercury isotope ratios in twenty-two lake sediment cores collected from various regions of the world. Tables exhibit age dating methods reported by individual authors for all lake sediment cores, analytical uncertainty of standard reference materials, wet mercury deposition fluxes and watershed area to lake area ratio reported by individual authors. Statistical test results of the compiled lake sediment core data are also presented in tables. Three figures are included to show histograms from normality tests for all data, spatiotemporal changes in Δ^{200}Hg from pre-industrial to present-day period and temporal changes in THg concentration in the lake sediment cores.

Reference	Sediment core	Age dating method
Cooke et al. (2013)	El Junco Laguna Negrilla	^{210}Pb, ^{14}C (Blaauw, 2010)
Gray et al. (2013)	Lake Ballinger	^{210}Pb, ^{226}Ra, ^{137}Cs (Fuller et al., 1999; Appleby & Oldfield, 1992)
Guédron et al. (2016)	Lake Luitel	^{210}Pb, ^{137}Cs (Appleby & Oldfield, 1978; Golberg, 1963)
Kurz et al. (2019)	Lost Lake	^{210}Pb, ^{226}Ra, ^{137}Cs (Baskaran, 2016)
Ma et al. (2013)	Phantom Lake Cleaver Lake McLurg Lake	^{210}Pb (Appleby & Oldfield, 1978)
Yin et al. (2016a)	Lake Qinghai Nam Co	^{210}Pb, ^{226}Ra, ^{137}Cs, ^{241}Am (reported by Lami et al., 2010 and Li et al., 2014 using ^{201}Pb-dating techniques by Appleby & Oldfield, 1978)
Yin et al. (2016b)	Lake Michigan (MI-116) Lake Michigan (MI-112) Lake Michigan (MI-50)	Sediment age calculated using the mass sedimentation rates (g cm^{-2} yr^{-1}) reported for Lake Michigan based on ^{201}Pb-dating techniques by Klump et al. (1997) and Song et al. (2005)
Lepak et al. (2020b)	Sapsucker Goldeneye Perfect Tomtit Locator Dunnigan Rectangle Square Clever	^{210}Pb (Appleby, 2002; Eakins & Morrison, 1978)

Table S1. Age dating methods reported by individual authors for all lake sediment cores compiled in this study.

Reference	n	δ^{202}Hg 2SD (‰)	Δ^{199}Hg 2SD (‰)	Δ^{200}Hg 2SD (‰)
Cooke et al. (2013)	6	0.08	0.04	NA
Gray et al. (2013)	30	0.08	0.05	0.05
Guédron et al. (2016)	NA	0.16	0.08	NA
Kurz et al. (2019)	11	0.09	0.02	0.04
Ma et al. (2013)	24	0.07	0.07	0.06
Yin et al. (2016a)	12	0.17	0.08	0.05
Yin et al. (2016b)	11	0.11	0.08	NA
Lepak et al. (2020b)	NA	0.05	0.05	0.03
Average		0.09	0.06	0.05

Table S2. Analytical uncertainty (2SD) of NIST RM 8610 (also known as UM-Almadèn) reported by individual authors.

		Shapiro-Wilk		
		Statistic	**df[a]**	***p*-value**
THg concentration (ng/g)				
All		0.214	251	<0.001
Pre-industrial		0.740	148	<0.001
Modern		0.329	103	<0.001
	Remote	0.939	56	0.007
	Unremote	0.485	47	<0.001
δ^{202}Hg				
All		0.836	232	<0.001
Pre-industrial		0.847	138	<0.001
Modern		0.762	94	<0.001
	Remote	0.833	47	<0.001
	Unremote	0.840	47	<0.001
Δ^{199}Hg				
All		0.971	232	<0.001
Pre-industrial		0.951	138	<0.001
Modern		0.964	94	0.011
	Remote	0.908	47	0.001
	Unremote	0.845	47	<0.001
Δ^{200}Hg				
All		0.962	199	<0.001
Pre-industrial		0.952	122	<0.001
Modern		0.916	77	<0.001
	Remote	0.940	45	0.022
	Unremote	0.940	32	0.72

[a] Abbreviation: Degree of freedom

Table S3. Shapiro-Wilk results from normality tests using SPSS for all data used in this study.

Sediment core (Reference)	Variables	n	r^2	Slope	*p*-value	Sediment core (Reference)	Variables	n	r^2	Slope	*p*-value
El Junco (Cooke et al., 2013)	THg	24	0.79	0.189	<0.0001	Lake Michigan (MI-112) (Yin et al., 2016b)	THg	13	0.67	0.573	0.001
	$\delta^{202}Hg$	6	0.78	0.002	0.020		$\delta^{202}Hg$	13	0.38	0.001	0.026
	$\Delta^{199}Hg$	6	0.55	0.001	0.092		$\Delta^{199}Hg$	13	0.04	-1E-04	0.519
Laguna Negrilla (Cooke et al., 2013)	THg	47	0.60	-0.726	<0.0001	Lake Michigan (MI-50) (Yin et al., 2016b)	THg	17	0.73	2.222	<0.0001
	$\delta^{202}Hg$	8	0.56	-0.002	0.034		$\delta^{202}Hg$	17	0.84	0.004	<0.0001
	$\Delta^{199}Hg$	8	0.57	0.001	0.031		$\Delta^{199}Hg$	17	0.32	-3E-04	0.017
Lake Ballinger (Gray et al., 2013)	THg	15	0.60	1.002	0.001	Sapsucker (Lepak et al., 2020a)	THg	27	0.22	0.165	0.015
	$\delta^{202}Hg$	15	0.74	0.006	<0.0001		$\delta^{202}Hg$	27	0.26	0.001	0.006
	$\Delta^{199}Hg$	15	0.70	0.002	<0.0001		$\Delta^{199}Hg$	27	0.32	0.001	0.002
Phantom Lake (Ma et al., 2013)	THg	19	0.59	135.6	1E-04	Goldeneye (Lepak et al., 2020a)	THg	22	0.68	0.403	<0.0001
	$\delta^{202}Hg$	19	0.80	0.006	<0.0001		$\delta^{202}Hg$	22	0.03	2E-04	0.434
	$\Delta^{199}Hg$	19	0.45	-0.001	0.002		$\Delta^{199}Hg$	22	0.46	4E-04	5E-04
Cleaver Lake (Ma et al., 2013)	THg	14	0.65	11.68	5E-04	Perfect (Lepak et al., 2020a)	THg	28	0.43	0.067	2E-04
	$\delta^{202}Hg$	14	0.51	0.006	0.004		$\delta^{202}Hg$	28	0.01	9E-05	0.589
	$\Delta^{199}Hg$	14	0.20	-4E-04	0.106		$\Delta^{199}Hg$	28	0.32	3E-04	0.002
McLurg Lake (Ma et al., 2013)	THg	16	0.70	1.994	<0.0001	Tomtit (Lepak et al., 2020a)	THg	17	0.73	0.793	<0.0001
	$\delta^{202}Hg$	16	0.82	0.008	<0.0001		$\delta^{202}Hg$	17	0.28	0.001	0.029
	$\Delta^{199}Hg$	16	0.03	9E-05	0.539		$\Delta^{199}Hg$	17	0.77	0.001	<0.0001
Lake Luitel (Guédron et al., 2016)	THg	23	0.30	1.333	0.006	Locator (Lepak et al., 2020a)	THg	36	0.82	0.542	<0.0001
	$\delta^{202}Hg$	23	0.10	0.001	0.146		$\delta^{202}Hg$	36	0.40	0.001	<0.0001
	$\Delta^{199}Hg$	23	0.31	0.002	0.005		$\Delta^{199}Hg$	36	0.57	0.001	<0.0001
Lost Lake (Kurz et al., 2019)	THg	24	0.71	0.155	<0.0001	Dunnigan (Lepak et al., 2020a)	THg	33	0.71	0.366	<0.0001
	$\delta^{202}Hg$	24	0.72	0.001	<0.0001		$\delta^{202}Hg$	33	0.72	0.001	<0.0001
	$\Delta^{199}Hg$	24	0.73	0.001	<0.0001		$\Delta^{199}Hg$	33	0.90	0.001	<0.0001
Lake Qinghai (Yin et al., 2016a)	THg	11	0.75	0.564	0.001	Rectangle (Lepak et al., 2020a)	THg	27	0.73	0.299	<0.0001
	$\delta^{202}Hg$	11	0.57	0.004	0.007		$\delta^{202}Hg$	27	0.08	3E-04	0.158
	$\Delta^{199}Hg$	11	0.64	4E-04	0.003		$\Delta^{199}Hg$	27	0.46	4E-04	1E-04
Nam Co (Yin et al., 2016a)	THg	34	0.59	0.102	<0.0001	Square (Lepak et al., 2020a)	THg	23	0.62	0.459	<0.0001
	$\delta^{202}Hg$	34	0.38	0.007	1E-04		$\delta^{202}Hg$	23	0.32	0.001	0.005
	$\Delta^{199}Hg$	34	0.56	5E-04	<0.0001		$\Delta^{199}Hg$	23	0.58	5E-04	<0.0001
Lake Michigan (MI-116) (Yin et al., 2016b)	THg	58	0.84	7.953	<0.0001	Clever (Lepak et al., 2020a)	THg	20	0.68	1.758	<0.0001
	$\delta^{202}Hg$	58	0.55	0.005	<0.0001		$\delta^{202}Hg$	20	0.36	0.001	0.005
	$\Delta^{199}Hg$	58	0.00	4E-05	0.649		$\Delta^{199}Hg$	20	0.77	0.002	<0.0001

Table S4. Results from the two-tailed conventional linear trend test.

Variables	n	H	*p*-value
Present-day vs Pre-industrial			
THg	268	74.43	< 0.05
$\delta^{202}Hg$	232	30.31	< 0.05
$\Delta^{199}Hg$	232	30.69	< 0.05
$\Delta^{200}Hg$	199	7.36	< 0.05
Present-day remote vs Present-day unremote			
THg	103	44.68	< 0.05
$\delta^{202}Hg$	94	0.08	0.77
$\Delta^{199}Hg$	94	3.49	0.06
$\Delta^{200}Hg$	77	15.92	< 0.05
Dunnigan, Square, Locator, Lost, El Junco vs other remote lakes			
$\delta^{202}Hg$	47	34.50	< 0.05
$\Delta^{199}Hg$	47	19.22	< 0.05
$\Delta^{200}Hg$	45	24.95	< 0.05

Table S5. Results from the Kruskal-Wallis test.

Reference	Sediment core	Wet mercury deposition flux (μg/m^2/yr)	Watershed: lake area ratio	Notes
Cooke et al. (2013)	El Junco	11.7	2.17	Zhang et al. (2014)
	Laguna Negrilla	11.7	5.33	Cooke et al. (2009)
Gray et al. (2013)	Lake Ballinger	11.4	34.3	Gray et al. (2013)
Ma et al. (2013)	Phantom Lake	3.72	2.24	Ma et al. (2013)
	Cleaver Lake	3.72	2.03	
	McLurg Lake	3.33	2.13	
Guédron et al. (2016)	Lake Luitel	6.73	159	Guédron et al. (2016)
Kurz et al. (2019)	Lost Lake	8.15	2.06	Kurz et al. (2019)
Yin et al. (2016a)	Lake Qinghai	1.66	6.77	Yin et al. (2016a)
	Nam Co	1.85	5.53	
Yin et al. (2016b)	Lake Michigan (MI-116)	3.15	2.03	Wikipedia
	Lake Michigan (MI-112)	3.15	2.03	
	Lake Michigan (MI-50)	3.15	2.03	
Lepak et al. (2020b)	Sapsucker	3.73	13.29	Lepak et al. (2020)
	Goldeneye	3.73	15.20	
	Perfect	1.5	1.20	
	Tomtit	4.62	8.24	
	Locator	7.73	8.20	
	Dunnigan	7.73	1.98	
	Rectangle	3.73	8.81	
	Square	9.4	2.76	
	Clever	4.62	2.24	

Table S6. Wet mercury deposition fluxes from Lepak et al. (2020) and Mulvaney et al. (2020) simulated by a global scale atmospheric chemistry transport model (GEOS-Chem) and the watershed area to lake area ratio reported by individual authors. Notes indicate references for the watershed:lake area ratios.

Reference	Sediment core	r^2	*p*-value
Cooke et al. (2013)	El Junco	0.88	< 0.05
	Laguna Negrilla	0.74	< 0.05
Gray et al. (2013)	Lake Ballinger	0.76	< 0.05
Ma et al. (2013)	Phantom Lake	0.86	< 0.05
	Cleaver Lake	0.83	< 0.05
	McLurg Lake	0.79	< 0.05
Guédron et al. (2016)	Lake Luitel	0.25	< 0.05
Kurz et al. (2019)	Lost Lake	0.72	< 0.05
Yin et al. (2016a)	Lake Qinghai	0.15	0.24
	Nam Co	0.36	< 0.05
Yin et al. (2016b)	Lake Michigan (MI-116)	0.93	< 0.05
	Lake Michigan (MI-112)	0.76	< 0.05
	Lake Michigan (MI-50)	0.88	< 0.05
Lepak et al. (2020b)	Sapsucker	0.21	< 0.05
	Goldeneye	0.03	0.49
	Perfect	0.03	0.42
	Tomtit	0.45	< 0.05
	Locator	0.31	< 0.05
	Dunnigan	0.52	< 0.05
	Rectangle	0.07	0.19
	Square	0.23	< 0.05
	Clever	0.42	< 0.05

Table S7. Statistical results on the negative correlations between 1/THg and δ^{202}Hg in the sediment cores.

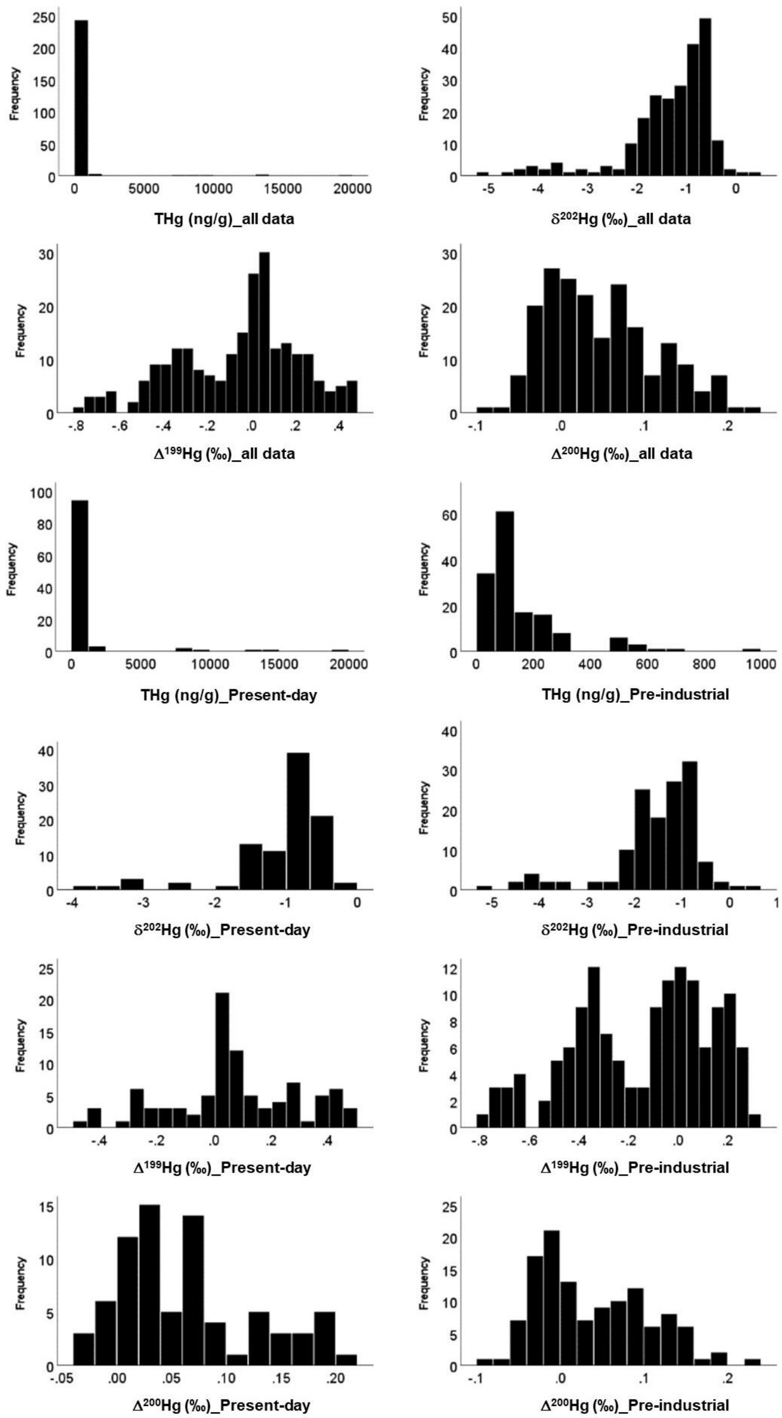

Figure S1. Histograms from normality tests using SPSS for all data used in this study.

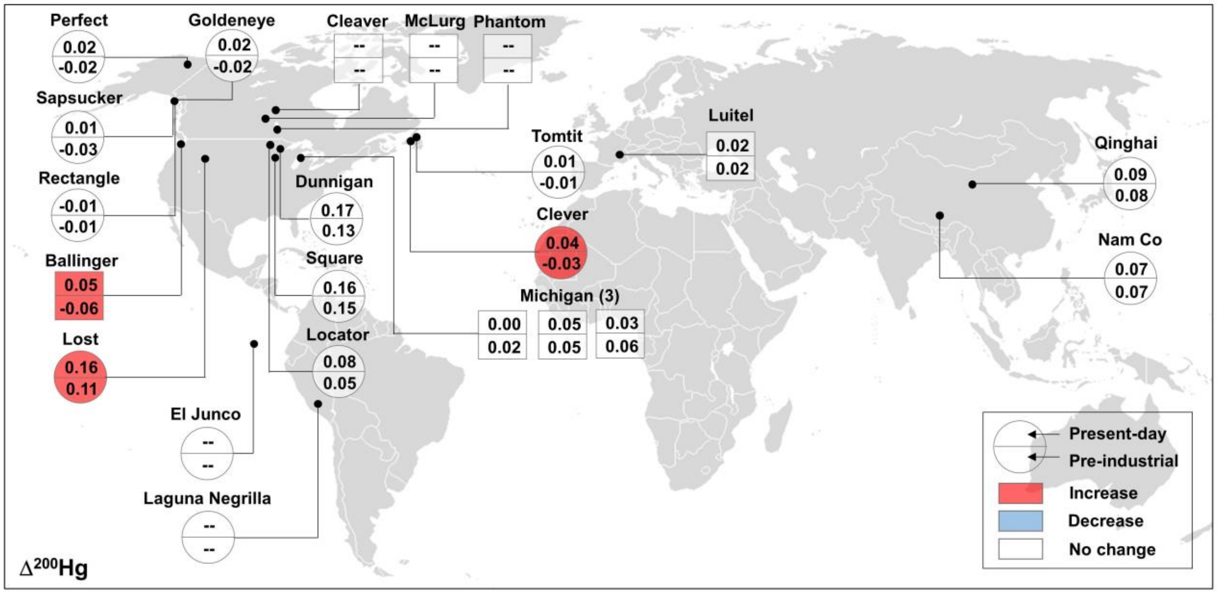

Figure S2. Spatiotemporal changes in Δ^{200}Hg (‰) from pre-industrial to present-day period in all lake sediment cores. The sediment cores shown in circles represent remote sites and the remaining sediment cores in squares represent unremote sites.

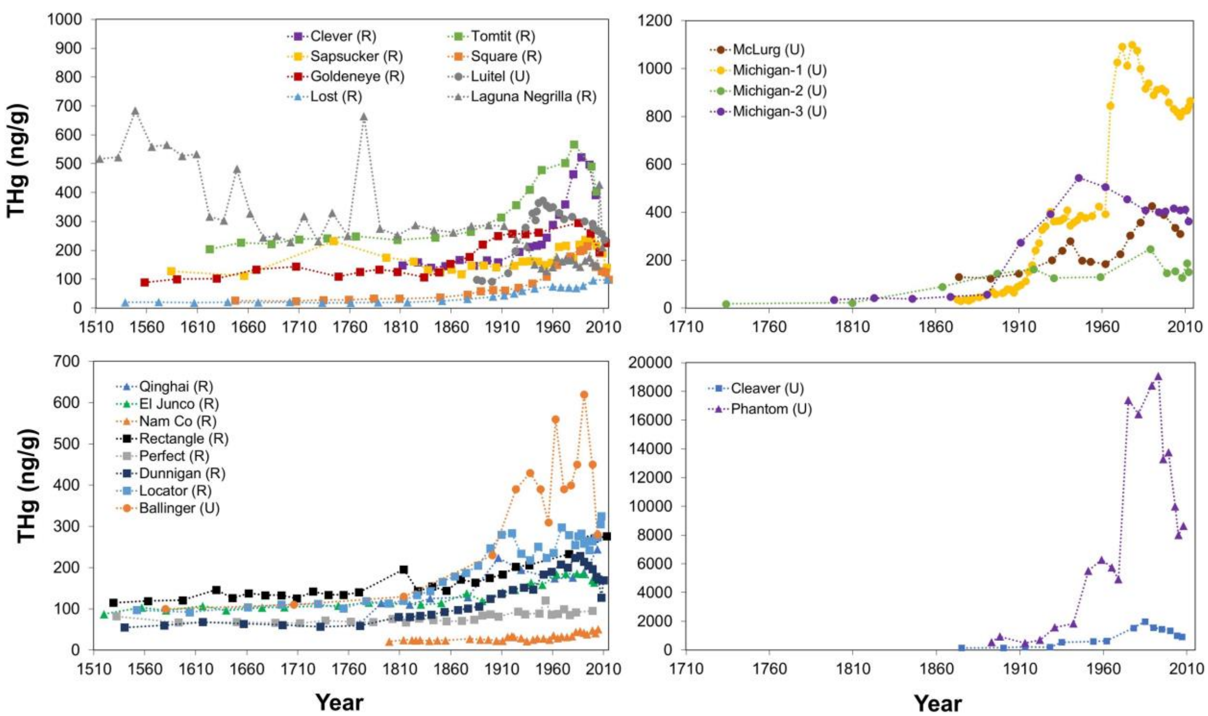

Figure S3. Temporal changes in THg concentration (ng/g) in the sediment cores.